Concentration Dependent Cu^{2+} Induced Aggregation and Dityrosine Formation of the Alzheimer's Disease Amyloid-β Peptide†

David P. Smith,[‡,§,||] Giuseppe D. Ciccotosto,[‡,§,⊥] Deborah J. Tew,[‡,§,⊥] Michelle T. Fodero-Tavoletti,[‡,§,⊥] Timothy Johanssen,[‡,§,⊥] Colin L. Masters,[‡,§] Kevin J. Barnham,[‡,§,⊥] and Roberto Cappai*[,‡,§,⊥,||,#]

Department of Pathology, The University of Melbourne, Victoria, 3010, Australia, Bio21 Institute, The University of Melbourne, Victoria, 3010, Australia, Centre for Neuroscience, The University of Melbourne, Victoria, 3010, Australia, Victoria, 3010, Australia, and The Mental Health Research Institute of Victoria, Parkville, Victoria 3052, Australia

Received October 9, 2006; Revised Manuscript Received December 29, 2006

ABSTRACT: The Amyloid β peptide (Aβ) of Alzheimer's diseases (AD) is closely linked to the progressive cognitive decline associated with the disease. Cu^{2+} ions can induce the *de novo* aggregation of the Aβ peptide into non-amyloidogenic aggregates and the production of a toxic species. The mechanism by which Cu^{2+} mediates the change from amyloid material toward Cu^{2+} induced aggregates is poorly defined. Here we demonstrate that the aggregation state of Aβ1−42 at neutral pH is governed by the Cu^{2+}:peptide molar ratio. By probing amyloid content and total aggregation, we observed a distinct Cu^{2+} switching effect centered at equimolar Cu^{2+}:peptide ratios. At sub-equimolar Cu^{2+}:peptide molar ratios, Aβ1−42 forms thioflavin-T reactive amyloid; conversely, at supra-equimolar Cu^{2+}:peptide molar ratios, Aβ1−42 forms both small spherical oligomers approximately 10−20 nm in size and large amorphous aggregates. We demonstrate that these insoluble aggregates form spontaneously via a soluble species without the presence of an observable lag phase. In seeding experiments, the Cu^{2+} induced aggregates were unable to influence fibril formation or convert into fibrillar material. Aged Cu^{2+} induced aggregates are toxic when compared to Aβ1−42 aged in the absence of Cu^{2+}. Importantly, the formation of dityrosine crosslinked Aβ, by the oxidative modification of the peptide, only occurs at equimolar molar ratios and above. The formation of dityrosine adducts occurs following the initiation of aggregation and hence does not drive the formation of the Cu^{2+} induced aggregates. These results define the role Cu^{2+} plays in modulating the aggregation state and toxicity of Aβ1−42.

Alzheimer's disease (AD)[1] is characterized by the abnormal accumulation of the Amyloid-β (Aβ) peptide (*1*). The Aβ peptide is cleaved from the membrane-bound amyloid precursor protein and subsequently aggregates into insoluble extracellular amyloid plaques that are a major pathological hallmark of AD (*1*). It is unclear whether the amyloid plaques are themselves toxic or represent the clearance or sequestration of a toxic species.

Transition metals such as copper (Cu), iron (Fe), and zinc (Zn) are present at high concentrations in Aβ plaques (Cu $\sim$ 400 μM, Zn $\sim$ 1 mM, and Fe $\sim$ 1 mM) and have been implicated as a significant pathological risk factor in AD (*2*−*5*). In addition, Cu^{2+} is released from cortical synaptosomes upon depolarization with K^+ with a minimal Cu^{2+}-concentration of 100 μM being observed in the synaptic cleft (*6*). This raises the possibility that the oxidative stress observed in AD patients is related to the production of reactive oxygen species (ROS) by metal-bound forms of Aβ (*7*−*10*). This hypothesis is supported by a number of independent observations. Neurofibrillary tangles and senile plaques isolated from AD brains are capable of generating toxic ROS that are dependent on the presence of Cu^{2+} and Fe^{3+} (*11*). The solublization of Aβ from post-mortem AD brain tissue is increased in the presence of metal chelators such as *N*,*N*,*N*′,*N*′-tetrakis (2-pyridyl-methyl) ethylene diamine and bathocuproine (*12*). Amyloid precursor protein transgenic mice treated orally with clioquinol, a moderate Cu^{2+}/Zn^{2+} chelator, resulted in a decrease in Aβ deposition (*13*). Moreover, a small phase II clinical trial with clioquinol showed efficacy in the severely affected AD group (*14*). Cu^{2+} loaded Aβ is toxic to primary cortical neurons (*15*−*17*) and is a potent inhibitor of the mitochondrial electron transport chain complex cytochrome *c* oxidase (also known as Complex IV) (*18*).

The coordination environment of Cu^{2+} bound to Aβ, as determined by electron paramagnetic resonance (EPR), Raman, and NMR spectroscopies, all showed that the ligand donor set of Aβ coordinating Cu^{2+} consists of the three histidine residues (His6, His13, and His14) and an as yet

† This work was funded by the Wellcome Trust, National Health and Medical Research Council of Australia, Australian Research Council and Prana Biotechnology Ltd. D.P.S. is a Wellcome Traveling Fellow.

* To whom correspondence should be addressed. Phone: (+61-3) 8344-2556. Fax: (+61-3) 9347-6750. E-mail: r.cappai@unimelb.edu.au.

‡ Department of Pathology, The University of Melbourne.

§ The Mental Health Research Institute of Victoria.

|| Current address: Institute of Molecular and Cellular Biology University of Leeds, Leeds, UK.

⊥ Bio21 Institute, The University of Melbourne.

Centre for Neuroscience, The University of Melbourne.

[1] Abbreviations: Aβ, Amyloid β peptide; AD, Alzheimer's diseases; EPR, electron paramagnetic resonance; EM, electon microscopy; Gdn.SCN, guanidine thiocyanate; ROS, reactive oxygen species; ThT, thioflavin-T.

10.1021/bi0620961 CCC: $37.00 © 2007 American Chemical Society
Published on Web 02/13/2007

undefined fourth ligand. The identity of the fourth ligand includes tyrosine at position 10 (Tyr10) (*16*, *19*−*21*), the N-terminal nitrogen (*22*), or an undefined carboxylate side chain (*23*). Our EPR studies indicate that increasing the Cu^{2+} above ~0.3 mol/mol peptide-induced line broadening in the Cu^{2+} EPR spectra suggests the presence of dipolar or exchange effects (*17*, *19*). These effects are observed when two Cu^{2+} ions are within 6.2 Å of each other, and we suggest that Aβ coordinates a second Cu^{2+} atom in a cooperative manner via a histidine bridge (*17*).

Cu^{2+} and Zn^{2+} ions are known to induce *de novo* aggregation of the Aβ peptide and the Cu^{2+} induced aggregates produced *in vitro* display enhanced toxicity toward primary cortical neurons (*16*, *24*). Metal bound forms of Aβ1−40 appear non-amyloidogenic (*25*) and are incapable of extending preformed amyloid seeds at Cu^{2+}:peptide molar ratios of 0.6 and above (*26*). Cu^{2+} induced aggregates of Aβ1−40/42 can be disaggregated by the use of chelators indicating that coordination of the metal ion is critical for stabilizing these aggregates (*26*, *27*). Metal coordination is saturated at Cu^{2+}:peptide molar ratios of 2.59:1 ± 0.17 for Aβ1−42, resulting in maximal peptide aggregation. Minimal precipitation is observed at a Cu^{2+}:peptide molar ratios of 0.25:1 ± 0.18 at pH 7.4 (*27*). The mechanism by which Cu^{2+} mediates the change from amyloid material toward the production of Cu^{2+} induced aggregates is not well defined. A critical factor that may govern the switch between these two states is the Cu^{2+}:peptide molar ratio. However, the effect of the Cu^{2+} concentration on the aggregation of the more pathologically significant Aβ1−42 species has not been determined. Given that Cu homeostasis is disrupted in AD this is an important and highly relevant issue to address (*28*, *29*). In this paper we investigated how the Cu^{2+}:peptide molar ratio affects the final aggregation state of Aβ1−42, the morphological characteristics of the resulting aggregates and the mechanisms which modulate their formation. The switch between amyloid material and the Cu^{2+} induced aggregates is centered at equimolar Cu^{2+}:peptide ratios and Cu^{2+} aggregation proceeds spontaneously, possibly via a collapsed monomeric state. Once formed, these aggregates appear incapable of extension or conversion into amyloid material. Only aged Aβ1−42 prepared at a Cu^{2+}:peptide ratio of 1:1 is neurotoxic. By comparison aged Cu^{2+} free Aβ is significantly nontoxic when aged. We also examined the conditions leading to the formation of the oxidative stress marker dityrosine and determined how this relates to the aggregation state of Aβ1−42.

MATERIALS AND METHODS

Peptide and Aggregate Preparation. Buffer A is defined as 10 mM sodium phosphate; 150 mM NaCl at pH 7.4. 25 mM Cu^{2+} was prepared as 1 part $CuCl_2$ to 6 parts glycine (Gly) in H_2O. The addition of a glycine counterion was essential to prevent the formation of insoluble phosphate−metal complexes. Aβ1−42 working solutions were prepared as described previously (*30*). For the aggregation experiments, $CuCl_2$/Gly was added to the Aβ1−42 (final concentration 10 μM) reaction mixture at the required concentration from the 25 mM stock solution. Samples were incubated at 37 °C with agitation at 200 rpm for the required time.

Electron Microscopy. Samples (10 μL) of aggregated protein were spotted onto carbon-coated copper grids for 30 min (ProSciTech). The grids were blotted with filter paper to remove excess buffer and the sample was stained with 0.5% (w/v) uranyl acetate for 30−40 s. Grids were blotted again and air-dried before analysis on a Siemens 102 transmission electron microscope, operating with a voltage of 60 kV.

Native/SDS−PAGE and Western Blotting. Samples were analyzed on 15% native or SDS/polyacrylamide gels using a Tris/tricine buffer system. After electrophoresis, Aβ1−42 was electrophoretically transferred onto nitrocellulose membrane, blocked with milk (10% w/v) and then probed with a monoclonal antibodies (either WO2 (*31*), 4G8 (Chemicon) or G211 (*31*)). The membranes were incubated with a secondary polyclonal rabbit anti-(mouse IgG) Ig conjugated to horseradish peroxidase (Amersham Pharmacia Biotech) and developed by the ECL detection system (Amersham Pharmacia Biotech).

Quantification of Aggregation and Fibril Formation. For determination of fibril growth endpoints, an aliquot (20 μL) was removed from the aggregation reaction and added to 600 μL of 20 μM thioflavin-T (ThT) solution at pH 7.4 in buffer A. The ThT signal was quantified by averaging the fluorescence emission at 480 nm over 10 s when excited at 444 nm using a Perkin-Elmer LS55 Fluorescence Spectrophotometer. To assay total aggregation, a discontinuous 90° light scattering assay was used. Aβ1−42 (500 μL, final concentration 10 μM), incubated for 24 h at 37 °C with agitation in the presence of a range of Cu^{2+}/Gly concentrations, was placed in a quartz cell with a 1 cm path length. The ability of the solution to scatter light was quantified by using a Perkin-Elmer LS55 Fluorescence Spectrophotometer with an excitation wavelength of 300 nm and scanning the emission wavelengths from 580 to 620 nm. Maximum light scattering was observed and recorded at 600 nm.

To monitor fibril formation as a function of time, 400 μL of 10 μM Aβ1−42 was prepared in buffer A with 20 μM ThT. Samples were incubated at 37 °C with agitation at 1000 rpm for 2 h. At the appropriate time point, 150 μL of each sample was removed and pipetted into a black 96 well plate. The amount of amyloid material formed was quantified by ThT fluorescence using a Hidex Plate CHAMELEON II. In each case, the samples were normalized by subtracting the initial signal from each data point and taking ThT signal at the end of the reaction as unity.

Sedimentation Analysis of Aβ1−42 Aggregates. Following incubation, samples were transferred into polycarbonate tubes (7 × 20 mm polycarbonate tubes, Beckman) and centrifuged at 100,000 rpm for 20 min (TLA-100 ultracentrifuge, Beckman) at 4 °C. Supernatants were recovered and the pellets resuspended in 150 μL of buffer A. The original sample, the supernatant and pellet fraction were analyzed by SDS−PAGE and visualized by Western blotting as described above.

Aggregate Dissociation. Following sedimentation as above, pellets were resuspended in 6 M guanidine thiocyanate for 24 h at 37 °C. Samples were then analyzed by SDS−PAGE and visualized by Western blotting as described above.

Gel Permeation Chromatography. Prepacked Superdex 75 column (Amersham) was equilibrated in buffer A before determining the apparent size of the Aβ1−42 aggregates incubated at 50 μM at various peptide to Cu^{2+} ratios. A flow rate of 0.5 mL/min was maintained with a BioRad BioLogic

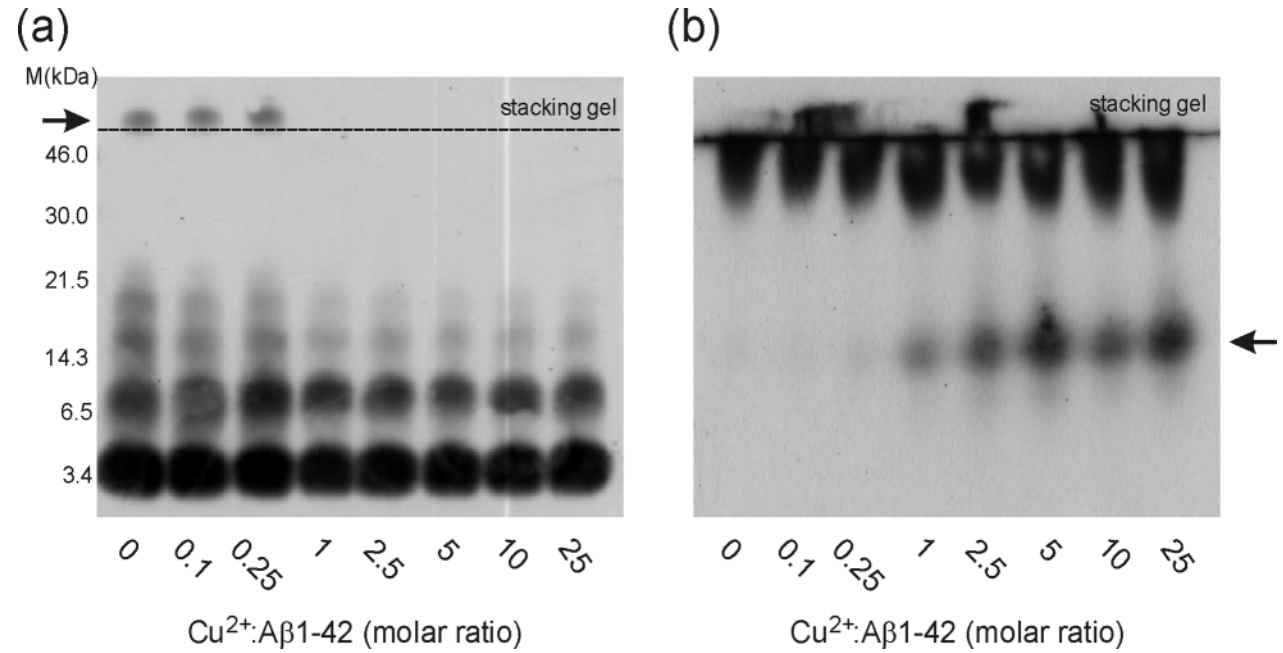

FIGURE 1: Analysis of Aβ1−42 Cu^{2+} aggregates by PAGE. (a) SDS−PAGE Western blot analysis; the arrow indicates the presence of aggregates that did not enter the gel matrix. (b) Native−PAGE Western blot analysis; the arrow indicates the presence of Cu^{2+} induced aggregates capable of entering the gel matrix.

workstation. The elutant was monitored using the absorbance at A_{280} nm. The columns were calibrated in buffer A with blue dextran (220 kDa), bovine serum albumin (66 kDa), carbonic anhydrase (29 kDa), cytochrome c (12.4 kDa), and aprotinin (6.5 kDa).

Dityrosine Formation. Peptide was prepared at 10 μM in the presence of 250 μM H_2O_2 at a range of Cu^{2+}:peptide molar ratios. After 24 h incubation at 37 °C with agitation at 200 rpm, the total fibril content was analyzed by ThT fluorescence, as above. The reaction was then quenched by the addition of 10 μL of 12.5 mM EDTA (final concentration 250 μM). Dityrosine content was quantified by using a Perkin-Elmer LS55 Fluorescence Spectrophotometer with an excitation wavelength of 320 nm and scanning the emission wavelengths from 350 to 500 nm. Maximum light signal was observed and recorded at 418 nm. For the continual growth experiment, 10 mL of 10 μM Aβ1−42, 25 μM Cu^{2+} was prepared as above with the addition of 250 μM H_2O_2. At each time point, 500 μL of the peptide sample was taken and the total aggregation was analyzed by light scattering. The reaction was quenched by the addition of 10 μL of 12.5 mM EDTA (final concentration 250 μM) and dityrosine content was quantified.

Primary Neuronal Cultures and Cell Viability Assay. Cortical neuronal cultures were prepared as described previously (*30*). The neuronal cells were allowed to mature for 6 days in culture before commencing treatment using freshly prepared serum-free neurobasal medium plus B27 supplements minus antioxidants. For the treatment of neuronal cultures, peptide was prepared at 50 μM at Cu^{2+}:peptide molar ratios of 0:1, 0.1:1, 1:1, and 10:1 and used either immediately or after aging for 24 h. Peptides were diluted to the final concentration of 5 μM in neurobasal medium. The mixtures were added to neuronal cells for 96 h. Cell survival was monitored by phase contrast microscopy, and cell viability was quantitated using the MTS assay as described previously (*30*). Briefly, the medium was replaced with fresh neurobasal medium supplemented with B27 lacking antioxidants, and 10% v/v MTS (Promega, Madison, WI) was added to each well and incubated for 3 h at 37 °C in a 5% CO_2 incubator. Plates were gently shaken and a 150 μL aliquot from each well was transferred to separate wells of a 96 well plate. The color change in each well was determined by measuring the absorbance at 490 nm using a Wallac Victor Multireader. Background readings of MTS incubated in cell-free medium were subtracted from each value before calculations. The data were normalized and calculated as a percentage of untreated vehicle control values. Data are shown as mean ± S.E. Statistical comparisons between groups were done using Student's *t* test.

RESULTS

Cu^{2+}:Peptide Molar Ratio Controls the Aggregation State of Aβ1−42. The mechanism by which Cu^{2+} mediates the change from amyloid material toward the production of Cu^{2+} induced aggregates is not well defined. A key factor that may govern the switch between these two states is the Cu^{2+}:peptide molar ratio. However, the effect of the Cu^{2+} concentration on the aggregation of the more pathologically significant Aβ1−42 peptide has not been determined. In this paper, we investigated how Aβ1−42 aggregation is affected by the Cu^{2+}:peptide molar ratio. Aβ1−42 (10 μM) was incubated at 37 °C for 24 h with agitation at 200 rpm. The resulting aggregates were analyzed by reducing SDS−PAGE and visualized by Western blotting using the antibody WO2, which recognizes Aβ residues 5−8 (Figure 1a). The gross morphology of the resulting aggregates was assessed by negative stain electron microscopy (EM) (Figure 2).

At sub-equimolar Cu^{2+}:peptide ratios, we observed the presence of large SDS resistant aggregates by reducing SDS−PAGE, which are incapable of entering the gel matrix (Figure 1a, arrow) along with a mixture of monomers to tetramers. These aggregates display characteristic fibril morphology by negative stain EM (Figure 2). A proportion

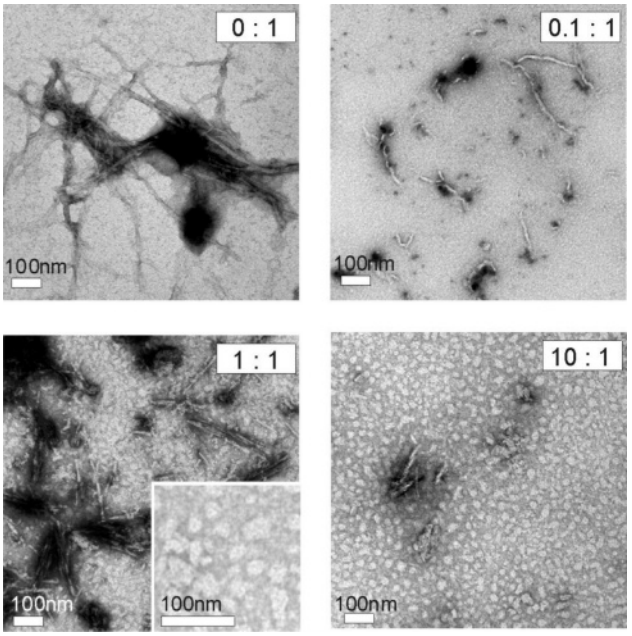

FIGURE 2: EM analysis of aggregated Aβ1−42 at a range of Cu^{2+}:peptide molar ratios. Scale bar, 100 nm. (Inset) Small spherical aggregates 10−25 nm in size present at a Cu^{2+}:peptide molar ratios of 1:1.

of these amyloid aggregates dissociate in SDS resulting in smaller oligomeric species that can enter the gel matrix (Figure 1a). At an equimolar Cu^{2+}:peptide ratio and above, the larger aggregated species observed by reducing SDS−PAGE were absent and only the lower molecular weight oligomers were present (Figure 1a). In addition, treatment of the insoluble sample pellet prepared in the absence of Cu^{2+} with 6 M guanidine thiocyanate (Gdn.SCN) results in the dissociation of the large SDS resistant aggregates, indicating that they are not an artifact of SDS treatment (Supplementary Figure 1). When analyzed under native, non-reducing conditions, all the Cu^{2+}:peptide ratios resulted in a substantial amount of high molecular weight material similar to that observed with SDS treatment at sub-equimolar peptide to Cu^{2+} ratios that migrates only slightly into the resolving gel matrix (Figure 1b). Nevertheless, at an equimolar Cu^{2+}:peptide ratio and above, there is a population of Aβ1−42 that can enter the resolving gel matrix (Figure 1b, arrow). Negative stain EM analysis shows the corresponding formation of Cu^{2+} induced spherical aggregates at 1:1 and 10:1 Cu^{2+}:peptide ratios, which are approximately 10−25 nm in size (Figure 2) along with large amorphous aggregates ranging in size from nm to μm (data not shown). These small spherical aggregates resemble early amyloid intermediates (*32*) or small diffusible globular oligomers (*33*). Under denaturing SDS conditions the Cu^{2+} induced aggregates break down into a mixture of monomers to tetramers (Figure 1a). However, under native conditions, the larger amorphous aggregates remain intact and do not enter the gel matrix. The species that does enter the gel matrix may represent the smaller spherical aggregates observed by EM which are only observed at equimolar ratios and above (Figure 1b, arrow).

To better understand the switch between these two distinct aggregate morphologies, the total amyloid content was assessed with the amyloid specific probe thioflavin-T (ThT) and total aggregation was measured by light scattering (Figure 3). When Aβ1−42 was incubated with increasing

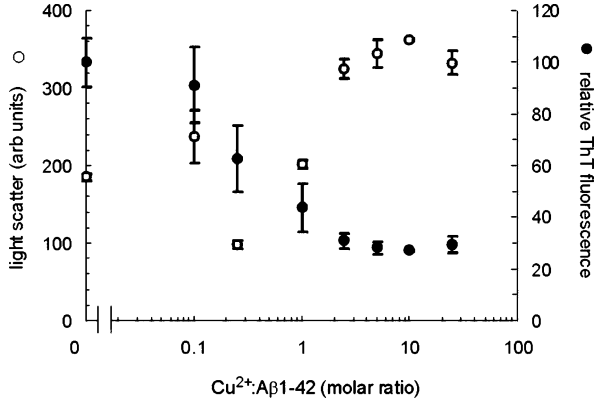

FIGURE 3: ThT and light-scattering analysis of Aβ1−42 aggregates at a range of Cu^{2+}:peptide molar ratios. The extent of amyloid formation was quantified by ThT fluorescence (●). The extent of total aggregation was quantified by light-scattering (○).

Cu^{2+} concentrations, there was a corresponding decrease in ThT fluorescence, indicating a loss of amyloidogenic material. The ThT signal was greatly diminished at Cu^{2+}:peptide molar ratios of 1:1 and above, the same point that the Cu^{2+} induced spherical aggregates were observed by EM. To determine if the loss in ThT signal was due to a reduction in amyloid material as opposed to the quenching of the ThT probe by the metal itself, the Cu^{2+} concentration was normalized to the highest concentration immediately before reading. Under these conditions, there was only slight quenching of the probe signal by the additional metal, indicating that the decrease in ThT fluorescence is due to a decrease in amyloid content (data not shown). We monitored the static light-scattering at 300 nm as an assessment of total aggregation and detected aggregated material with elevated Cu^{2+} levels. Scattering occurred at peptide molar ratios greater than 1:1, signifying the presence of material that scatters light but is only weakly ThT reactive. At close to equimolar Cu^{2+}:peptide ratios, both aggregate morphologies are clearly visible by EM (Figure 2), indicating that there are two mutually exclusive pathways of aggregation being controlled by the Cu^{2+} ratio. Accordingly, considerably less amyloid material is observed at supra-equimolar Cu^{2+}:peptide ratios by EM. Taken together, the data presented in Figures 1−3 demonstrate that there is a switch between the amyloid morphology and the Cu^{2+} induced aggregate morphology governed by the molar ratio between Cu^{2+} and peptide. Amyloid material is being preferentially produced at sub-equimolar Cu^{2+}:peptide molar ratios and Cu^{2+} induced non-amyloidogenic aggregates are generated at equimolar ratios and above.

Cu^{2+} Induced Aggregates are Insoluble. The solubility of the Cu^{2+} induced aggregates prepared after 24 h incubation was assessed by ultracentrifugation at 100 000 rpm. The initial sample, resulting supernatant and pellet fractions were assayed by ThT fluorescence and Western blot analysis (Figure 4). The Western Blot shows the 4 kDa band however, higher order oligomers were also present similar to those observed in Figure 1a. In all cases, the majority of the material partitioned into the pellet while the supernatant contained little detectable ThT fluorescence. Approximately ∼8−10% of total peptide was present in the supernatant in all samples as measured by A_{214} (data not shown). The Western blotting data indicated that a small amount of soluble Aβ peptide was detectable using either the 4G8 or G211

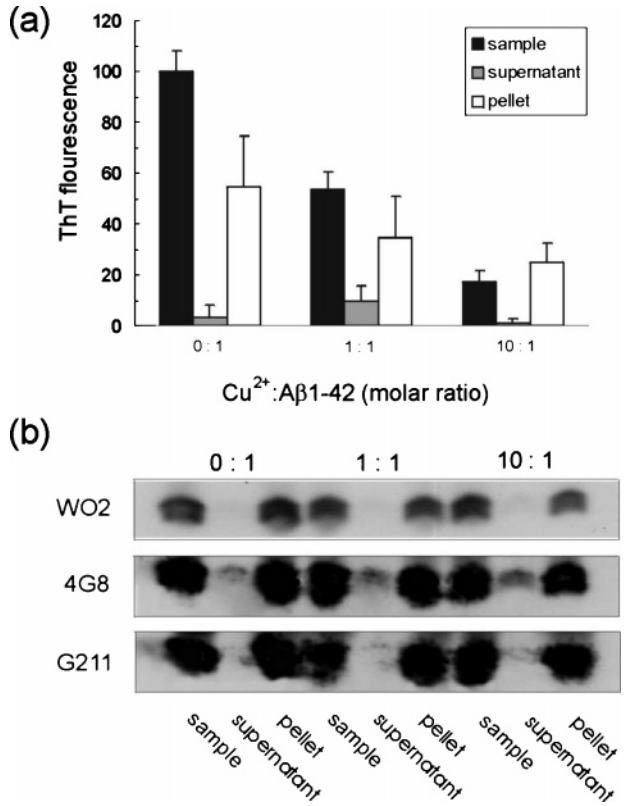

FIGURE 4: Sedimentation analysis on the solubility of Aβ1−42 aggregates formed at Cu^{2+}:peptide molar ratio of 0:1, 1:1, and 10:1. Samples were centrifuged at 100 000 rpm for 20 min, obtaining soluble supernatant and insoluble pellet fractions. (a) Proportion of amyloid material in each fraction was assed by ThT fluorescence. (b) Total peptide distribution was assessed by Western blot analysis. Samples were electrophoresed by SDS−PAGE and probed separately with WO2, 4G8, and G211 antibodies. The 4 kDa band is shown.

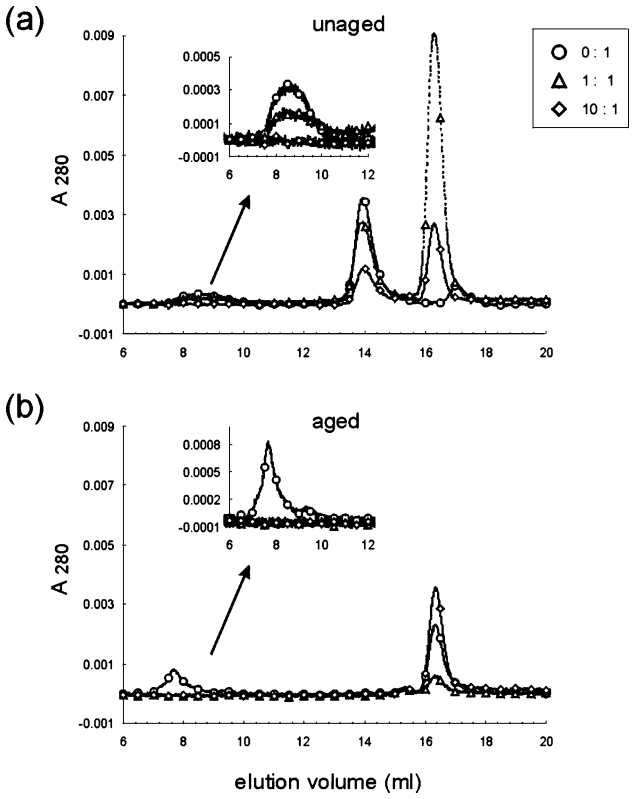

FIGURE 5: Gel permeation chromatography of Aβ1−42 both (a) fresh (5 min incubation) and (b) aged (24 h incubation) at Cu^{2+}:peptide molar ratio of 0:1 (○), 1:1 (△), and 10:1 (□) were analyzed by gel permeation chromatography. (Inset) Large oligomeric fractions eluting around the void volume. Samples were sized on a 10/30 Superdex 75 column running at 0.5 mL/min in buffer A. The eluant was monitored using absorbance at A_{280} nm. The columns were calibrated in buffer A with Blue Dextran (220 kDa), Bovine serum Albumin (66 kDa), Carbonic Anhydrase (29 kDa), Cytochrome C (12.4 kDa), and Aprotinin (6.5 kDa).

antibodies. However, longer exposure times with WO2 also showed a slight amount of soluble material in the supernatant. Nevertheless, the vast majority of the Aβ peptide resided in the pellet fractions. The ThT fluorescence and western blotting data indicated that after 24 h incubation the majority of the amyloid material and the Cu^{2+} induced aggregates, at all Cu^{2+}:peptide ratios, are insoluble.

Assessing the Oligomeric Nature of the Cu^{2+} Induced Aggregates. To define the processes taking place during the early stages of aggregation under native buffer conditions, samples of Aβ1−42 were analyzed by gel permeation chromatography on a 10/30 Superdex 75 column (Figure 5). Unaged Aβ1−42 in the absence of additional Cu^{2+} displayed peaks at elution volumes of 9 and 14 mL. The broad peak at 9 mL occurred just after the void volume (8 mL) and represents a range of oligomeric species with an approximate mass of ∼60−70 kDa (Figure 5, inset). The major peak migrated with an elution volume of 14.0 mL and was consistent with an approximate mass of ∼14−15 kDa, as measured against the globular protein standards. However, due to the unstructured nature of Aβ1−42, it is expected to have a higher hydrodynamic radius than globular proteins of the same MW. The migration of the Aβ peptide is also sensitive to the chromatographic conditions and can migrate with molecular weights ranging from 5 to 18 kDa depending on the column material and conditions used (*34*, *35*). It is therefore possible that this peak represents the monomeric state of the peptide. It is also possible that this peak represents both monomers and high order aggregates in rapid equilibrium. Upon aging, the major peak shifted from 14.0 to 16.3 mL, consistent with an approximate mass of ∼8 kDa, which may represent a collapsed form of the monomer. The larger oligomeric peak also shifted, from 9 to 8 mL, consistent with the formation of the larger amyloid fibrillar species observed by EM and ThT.

Unaged Aβ1−42 at an equimolar Cu^{2+}:peptide ratio showed the presence of three included peaks. The first was centered at 9 mL and represented an oligomeric species similar to those seen in the absence of Cu^{2+} (Figure 5, inset). A second peak can be observed at 14.0 mL and was similar in size to that seen in the absence of Cu^{2+}. The third larger peak was centered at 16.3 mL, with an approximate mass of ∼8 kDa as observed for aged Aβ1−42 in the absence of Cu^{2+}. Control experiments in which Cu^{2+} was added to a known amount of Aβ1−42 indicated that the addition of metal induced an exaggerated absorbance at A_{280}, accounting for the apparent large increase in peak size (data not shown). Comparable size exclusion profiles have been observed previously with freshly prepared Aβ1−40 in the presence of Cu^{2+}, displaying the formation of an apparently lower molecular weight species (*36*). Upon aging of Aβ1−42, the 16.3 mL peak height was greatly reduced, and presumably this species has formed into the larger aggregates that were observed in Figures 1 and 2 and are incapable of entering

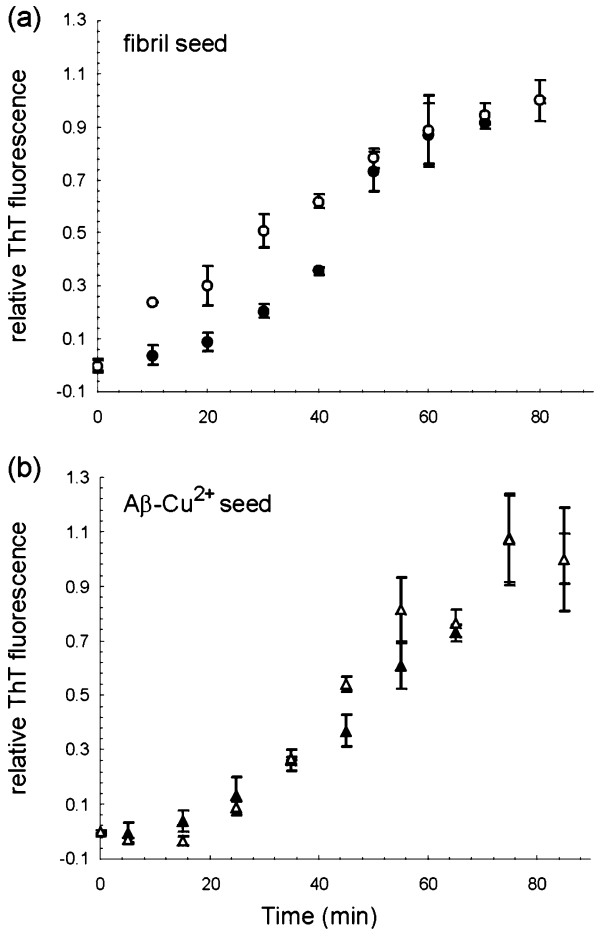

FIGURE 6: Growth of Aβ1−42 fibrils as monitored by ThT fluorescence in the presence or absence of 10% (v/v) preformed aggregated material. (a) Aβ1−42 at a Cu^{2+}:peptide molar ratio of 0:1 minus seed (●), Aβ1−42 in the absence of Cu^{2+}, with a 10% (v/v) seed of preformed Aβ1−42 fibrils prepared in the absence of Cu^{2+} (○). (b) Aβ1−42 (▲) 2.5 μM Cu^{2+} was added to this sample to compensate for the Cu^{2+} carried over by the Cu^{2+} induced seed material resulting in at Cu^{2+}:peptide molar ratio of 0.25:1 at time 0. Aβ1−42 at a Cu^{2+}:peptide molar ratio of 0.25:1, with a 10% (v/v) seed of preformed Cu^{2+} induced Aβ1−42 oligomers prepared at a Cu^{2+}:peptide molar ratio of 2.5:1 (△). NB − 2.5 μM Cu^{2+} was added to the sample to control for the Cu^{2+} carried over with the seed. In each case, samples were normalized by subtracting the initial signal from each data point and taking ThT signal at the end of the reaction as unity.

the column matrix. A similar distribution of oligomers was observed at the supra-equimolar Cu^{2+}:peptide ratio of 10:1. However, a small fraction of peptide persisted and eluted at 16.3 mL upon aging. These data indicate that the Cu^{2+} does not simply precipitate the Aβ1−42 from solution but rather there is a distinct aggregation pathway that proceeds via a small soluble species resulting in the larger insoluble aggregates observed by EM.

Cu^{2+} Induced Aggregates Do Not Accelerate Amyloid Formation. To ascertain if the Cu^{2+} induced aggregates are able to influence or accelerate amyloid formation seeding experiments were performed. To prepare the seed, 50 μM Aβ1−42 was aged for 24 h either in the absence of Cu^{2+} (0:1) or at a Cu^{2+}:peptide molar ratio of 2.5:1. Freeze-thawed aliquots were then used to seed unaged Aβ1−42 (minus Cu^{2+}) (Figure 6). Consistent with previous publications (*37*) seeding with preformed amyloidogenic Aβ1−42 reduced the lag phase and increased the rate of fibril formation (Figure 6a). If the Cu^{2+} induced aggregates can be extended into fibrillar material, then the addition of preformed Cu^{2+} induced aggregates should influence the rate of fibril formation in a similar manner. However, the preformed Cu^{2+} induced aggregate seeds caused no observable difference in the rates of fibril formation between the seeded and the non-seeded samples (Figure 6b). To compensate for the Cu^{2+} being carried over with the seed material, 2.5 μM Cu^{2+} was added to the control sample at time 0. The identical aggregation profile between the addition of Cu^{2+} ions or the addition of Cu^{2+} induced aggregates indicates that preformed Cu^{2+} aggregates cannot accelerate fibril formation. However, these results do not allow us to definitively conclude that the Cu^{2+} induced aggregates cannot form fibrils. It is feasible that these aggregates could dock together and convert into protofibrils and fibrils over an extended time period. To test this, samples of Cu^{2+} induced aggregates were incubated for 37 days and ThT fluorescence and aggregate morphology was monitored (Supplementary Figure 2). Over this time period, there was no change in either ThT fluorescence or aggregate morphology, suggesting this conversion did not occur. It is possible that even longer time periods (months to years) are required for these morphological changes to occur. It has also previously been demonstrated that Cu^{2+} treated Aβ1−40 dose not support fibril growth by docking to the ends of existing fibrils (*26*). These results, together with the observation of decreased ThT fluorescence (Figure 3) and alterations in aggregate morphology (Figures 2), indicate that the Cu^{2+} induced aggregates of Aβ1−42 represent an endproduct from an alternative aggregation pathway that is incapable of subsequent fibril formation on the short (hours) to medium (days) time scale used.

Aged Cu^{2+}Aggregates Are Toxic. We have previously demonstrated that unaged Aβ1−42 at a Cu^{2+}:peptide molar ratio of 1:1 and 1:10 is highly neurotoxic and this toxicity correlated with the formation of a histidine bridged dimer (*17*). Unaged Aβ1−42 at a Cu^{2+}:peptide molar ratios 0:1 and 0.1:1 also showed neurotoxic activity; however, this effect was diminished in comparison to the 1:1 and 10:1 molar ratios (*17*). It is unknown, however, what effect aging has on the neurotoxic activity of Cu^{2+} induced aggregates. To address this important issue, Aβ1−42 was aged for 24 h at Cu^{2+}:peptide molar ratios of 0:1, 0.1:1, 1:1, and 10:1. The resulting aggregates were tested for neurotoxic activity on mouse primary cortical cultures (Figure 7). Aging Aβ1−42 for 24 h either in the presence or absence of Cu^{2+} prior to adding it to the neurons resulted in an absence of neurotoxic activity for the 0:1, 0.1:1 and 10:1 Cu^{2+}:peptide molar ratios. However, Aβ1−42 prepared at a Cu^{2+}:peptide molar ratio of 1:1 showed significant neurotoxicity. These results in conjunction with our published data on unaged Aβ-Cu^{2+} complexes (*17*) would indicate that both early aggregated forms of metal loaded Aβ1−42 and aged aggregates at an equimolar ratio were highly toxic to neuronal cells. At supra-equimolar Cu^{2+}:peptide molar ratio (10:1), toxicity was lost upon aging. This loss in toxicity may be due to the formation of the large aggregates as observed by EM, which were presumably unable to interact with the neuronal cells. Amyloid-like material generated at sub-equimolar Cu^{2+}:peptide molar ratios of 0:1, 0.1:1 was also nontoxic to this cell line.

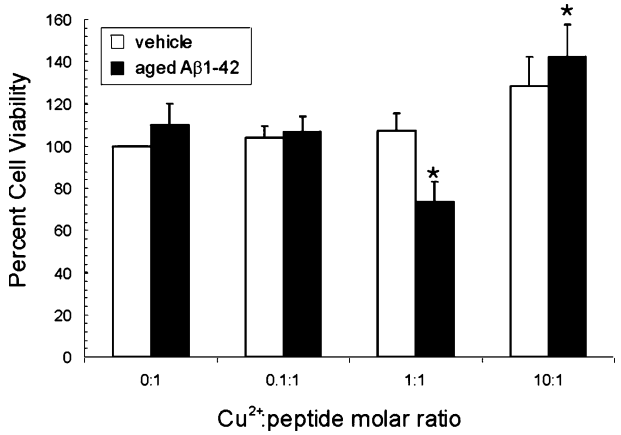

FIGURE 7: Toxicity of aged WT Aβ1−42 coordinated to Cu^{2+}. Primary cortical neurons were grown at low density (1.25×10^5 cells/cm^2) for 5 days, and the viability of these cells following peptide treatment was determined by measuring the inhibition of MTS reduction. Cortical neurons were treated with 5 μM peptide for 96 h in serum-free media. WT Aβ1−42 aged for 24 h at a range of Cu^{2+}:peptide molar ratios (■), vehicle control (□). Data are shown as mean ± S.E. Statistical comparisons between groups were done using Student's *t* test. p 0.05 versus vehicle; each experiment was carried out in triplicate.

Dityrosine Formation is Linked to Cu^{2+} Aggregate Formation. The production of ROS and subsequent oxidative stress has been implicated in the pathology of AD (*7*). A byproduct of these reactions are tyrosine radicals, which react with each other resulting in the formation of dityrosine cross-linked Aβ oligomers (*38*, *39*). To determine if dityrosine formation is linked to any specific aggregate form, 10 μM Aβ1−42 was incubated at 37 °C with agitation at 200 rpm for 24 h at a range of Cu^{2+}:peptide molar ratios in the presence of 250 μM H_2O_2. The addition of H_2O_2 strongly promotes dityrosine cross-linking via the increased production of ROS (*38*, *39*). Postincubation, the peptide aggregates were assayed for the presence of amyloid material and dityrosine content (Figure 8a). As noted above, increasing the Cu^{2+} concentration decreases ThT reactive amyloid material, with little change in the signal observed at greater than equimolar Cu^{2+}:peptide molar ratios. Interestingly, there was a decrease in the ThT signal in the presence of H_2O_2 as compared to its absence (Figure 3). This reduction presumably reflected the oxidative modification of a number of residues; in particular, Met35 resulting in increased solubility as Aβ peptides containing oxidized Met35 are known to be less fibrillogenic compared to wild-type Aβ (*40*, *41*). The formation of dityrosine closely mirrored the loss of amyloid material and corresponds to the formation of the Cu^{2+} induced aggregates (Figure 8) with maximal formation above equimolar Cu^{2+}:peptide ratios. Thus, conditions leading to the formation of the Cu^{2+} induced aggregates are also required for dityrosine formation.

The efficiency of dityrosine formation into fibrillar Aβ is known to be increased over that seen in monomeric Aβ (*42*). It has been suggested that small amounts of dityrosine formation may occur prior to the conversion of Aβ into amyloid, stabilizing early intermediates (*43*); conversely, formation of dityrosine may occur in a time-dependent manner post-aggregate formation (*38*). To define if dityrosine formation occurred pre- or post-aggregation and to better establish the mechanism of dityrosine formation, the aggregation and dityrosine formation of Aβ1−42 was monitored as a function of time (Figure 8b). As expected, Aβ1−42 aggregated without an observable lag phase, and aggregation was essentially complete after 15 min (Figure 8b, open circles). Control experiments in the absence of H_2O_2 gave an identical aggregation profiles (data not shown), indicating that H_2O_2 does not affect Cu^{2+} induced aggregation. Dityrosine formation also proceeded without a measurable lag phase and took approximately 60 min to reach completion (Figure 8b, closed circles). The rate of dityrosine formation was significantly slower than for total aggregate formation and is therefore a consequence of metal-induced aggregate formation.

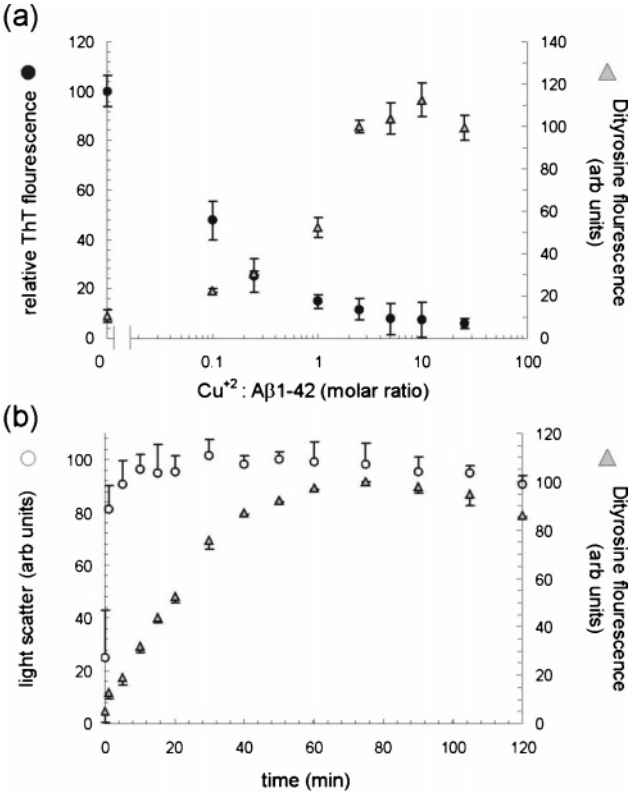

FIGURE 8: Formation of dityrosine cross linked Aβ by Cu^{2+} induced aggregation. (a) Formation of dityrosine as a function of Cu^{2+} concentration. Each sample was probed for total fibril content by ThT fluorescence (●) and dityrosine content (gray triangle). (b) Aggregation and dityrosine formation of 10 μM Aβ1−42 in the presence of 25 μM Cu^{2+} and 250 μM H_2O_2 as monitored by light-scattering (○) and dityrosine fluorescence spectroscopy (gray triangle) respectively.

DISCUSSION

Implications for the Aggregation of Aβ Peptide. The results presented here demonstrate that the *de novo* aggregation pathway of Aβ1−42 at neutral pH is governed by the molar ratio of Cu^{2+}:peptide in solution. By probing amyloid content using ThT fluorescence and the total aggregation by light scattering, we observed a distinct Cu^{2+} switching effect centered at equimolar Cu^{2+}:peptide ratios. At sub-equimolar ratios, Aβ1−42 formed ThT-reactive amyloid-like material that was highly stable and resistant to SDS denaturation after a short period of heating. In the presence of the stronger denaturant (Gdn.SCN), further solubilization of the peptide can be observed. Conversely, at supra-equimolar ratios, Aβ1−42 formed small insoluble spherical oligomers ap-

proximately 10−20 nm in size and large amorphous aggregates ranging in size from nm to μm, which are susceptible to SDS solubilization, suggesting they are less stable than amyloid-like material. Size-exclusion chromatography indicated that prior to the formation of the Cu^{2+} induced aggregates, the addition of Cu^{2+} ions to unaged peptide resulted in the formation of a transiently populated species consistent with a possible collapsed or more ordered monomeric state. It has previously been shown that CD spectra of Aβ1−28 titrated with Cu^{2+} has a structural transition from random coil to a more ordered conformation but not β-sheet (*22*). Formation of the Cu^{2+} induced aggregates did not result in ThT fluorescence, and the small observable signal can be attributed to the co-population of a small number of amyloid fibrils as observed by EM. We also observed little change in either ThT fluorescence or light scattering at Cu^{2+}:peptide ratios of 2.5:1 and above consistent with Aβ1−42 metal binding being saturated at 2.59:1 ± 0.17 (*27*). The coexistence of both the amyloid material and the Cu^{2+} induced aggregates would suggest two mutually exclusive aggregation pathways. At Cu^{2+}:peptide ratios of ∼0.3:1 and above, the Aβ peptide has been shown to form a histidine-bridged Cu^{2+} dimer, as observed by EPR, which is essential for the metal mediated toxic effect and the formation of this bridge appears to corresponds with the initial formation of the Cu^{2+} induced aggregates (*17*, *19*, *44*). However, variant peptide in which the formation of the His bridge was ablated still formed Cu^{2+} induced aggregates; hence, Cu^{2+} induced aggregation of Aβ is not dependent on the ability of the peptide to form a His bridge but on its ability to coordinate the initial Cu^{2+} (*17*).

It has been demonstrated here and elsewhere (*24*, *25*) that formation of Cu^{2+} induced aggregates by Aβ occurs spontaneously. We have demonstrated that Cu^{2+} induced aggregates of Aβ1−42 prepared at a peptide to Cu^{2+} ratio of 2.5:1 do not influence the rate amyloid formation. As a control, 2.5 μM Cu^{2+} was added to the unseeded reaction resulting in a Cu^{2+}:peptide molar ratio of 0.25:1. Presumably a small proportion of Cu^{2+} induced aggregates were formed spontaneously but they did not accelerate the rate of amyloid formation as compared to Aβ1−42 in the absence of Cu^{2+}, and the remaining peptide was left to form amyloid-like material. Cu^{2+} induced aggregates also appear unable to convert into amyloid material over an extended time frame. The effect of the Cu^{2+}:peptide molar ratio has been studied on the extension of the shorter Aβ species, Aβ1−40 (*26*). It was observed that after a 90 min incubation at a Cu^{2+}:peptide molar ratios of above 0.4:1, there was no observable extension of preformed Aβ1−40 fibrils. Slow fibril growth was seen at molar ratios of less than 0.6:1 after 2 days, whereas no extension of preformed amyloid material was observed at equimolar ratios (*26*). In accordance with our current data, the Aβ1−40 metal ion complexes were non-fibrillogenic in nature and lacked the ability to bind ThT (*26*). The data presented here makes the important finding that the switch between the two aggregation states is centered at an equimolar Cu^{2+}:peptide ratio in the absence of preformed material. In addition, our EM data shows that both the Cu^{2+} induced aggregates and amyloid material can coexist. Together with the Aβ1−40 findings (*26*), we suggest that as the Cu^{2+}:peptide ratio approaches 1:1 and above, the spontaneous formation of the Cu^{2+} induced aggregates causes the available Aβ peptide in solution to be rapidly depleted, and hence, formation of amyloid material is prevented both *de novo* and by the extension of preformed seeds. Trace metal ions such as Cu^{2+} are required for Aβ fibril formation as solutions depleted of metal ions do not form amyloid material (*45*). The addition of Cu^{2+}, Zn^{2+}, or Fe^{3+} to metal depleted solutions of Aβ1−40 accelerates amyloid formation in the same manner as seeding with monomeric Aβ1−42 (*45*). It is possible that at very low Cu^{2+} concentrations, the Aβ-metal ion complexes are required for amyloid formation by either acting as a nuclei or inducing structure with in the peptide (*10*). However at the Cu^{2+} concentrations used here these same amyloidogenic species/nuclei may become so highly populated that they aggregate via an alternative-pathway to form the Cu^{2+} induced aggregates. Once formed, these Cu^{2+} induced aggregates are then incapable of amyloid formation or conversion into amyloid material. Alternatively, they may extend or convert into amyloid material, at such a slow rate, that it is not observed on the time frame used here.

The different aggregated forms of the Aβ1−42 peptide were tested for their neurotoxic activity toward mouse primary cortical neurons. We have previously demonstrated that unaged Aβ1−42 at a Cu^{2+}:peptide molar ratio of 1:1 and 1:10 is highly toxic to neuronal cell lines, and this toxicity correlates with the formation of a histidine bridged dimer (*17*). Unaged Aβ1−42 at a Cu^{2+}:peptide molar ratios 0:1 and 0.1:1 also show a neurotoxic effect; however, this effect was greatly attenuated when compared to the 1:1 molar ratio. Here we demonstrate that when aged, only Aβ1−42 at Cu^{2+}:peptide ratio of 1:1 showed significant neurotoxic activity (Figure 7). This neurotoxic activity correlates with co-formation of Cu^{2+} induced aggregates and small amyloid-like fibrils. However, end stage fibrils alone and aggregates produced at a 10:1 Cu^{2+}:peptide ratio are shown to have little to no toxic effect at the concentrations used. The toxic species present here after aging may therefore represent a sub population of the soluble peptide which persists in solution only at equimolar ratios. At Cu^{2+}:peptide ratios of 0.1:1, the concentration of the toxic species is presumably much reduced compared to equimolar ratio due to the low metal concentration and hence does not reached a toxic threshold. At Cu^{2+}:peptide ratio of 10:1 the apparent lack of toxicity upon aging may, reflect the formation of the large amorphous aggregates as observed by EM resulting in the sequestering or loss of the toxic species, thus preventing interaction with the neuronal cells. *In vivo*, it is possible that the slow acumination of these Aβ-Cu^{2+} complexes leads to toxicity where as the alternative formation of amyloid material has a protective effect. It has been suggested that Aβ-Cu^{2+} complexes may impart their toxic effect via the production of ROS, resulting in oxidative stress, and this toxic mechanism has been implicated in the pathology of AD (*2*, *7*). The single Tyr10 residue located at or near the metal binding site of Aβ is a critical residue involved in its neurotoxic activity (*39*). Theoretical calculations, combined with experimental data, have demonstrated that the tyrosine radical drives the transfer of electrons required for the production of ROS (*39*). A byproduct of this reaction are tyrosine radicals that react with each other resulting in the formation of dityrosine cross-linked Aβ oligomers with increased structural strength and resistance to proteolysis (*35*), a characteristic feature of brain derived Aβ (*46*). *In vivo*, the

H_2O_2 required for this reaction to take place could originate from activated microglia, impaired mitochondrial function, or from the metal-bound forms of the Aβ peptide itself (*38*, *47*). It is unknown at present whether the dityrosine-linked Aβ itself or the radicals that are produced during its generation are toxic. The efficiency of dityrosine formation in fibrillar Aβ is greater than for monomeric Aβ (*42*). Dityrosine formation may occur prior to the conversion of Aβ into amyloid (*43*) alternatively dityrosine formation may occur in a time-dependent manner post aggregate formation (*38*). In this study, the dityrosine signal correlated strongly with the generation of the Cu^{2+} induced aggregates and occurred after the Cu^{2+} induced aggregates had formed and is therefore a consequence of metal-induced aggregation. At Cu^{2+}:peptide ratios of 0.6:1 and above, the Aβ peptide forms a histidine-bridged Cu^{2+} dimer (*17*, *19*, *44*). This bridging causes two Tyr residues from neighboring Aβ peptides to be brought close enough together in space to allow the short-lived tyrosine radicals to react and form a covalent bond. We and others have shown that Aβ in the presence of Cu^{2+} is highly toxic (Figure 7) (*8*, *17*, *48*, *49*) and Tyr10 is necessary for this neurotoxic activity because mutating Tyr10 in Aβ1−42 to Ala attenuates the production of ROS and prevents neurotoxicity (*39*).

The effect of Cu^{2+} binding and its role in aggregation has been implicated in other neurodegenerative diseases (*50*). For the prion protein, Cu^{2+} ions inhibit the aggregation of full-length recombinant prion protein into amyloid fibrils (*50*). Conversely, Cu^{2+} ions can accelerate the aggregation of α-synuclein without altering the fibrillar structure (*51*). Cu^{2+} coordination can affect the secondary and tertiary structures of peptide and proteins resulting in either a population of amyloidogenic precursor states or non-amyloidogenic species, which will significantly influence the morphology of the aggregate produced. In this current study, we have demonstrated that the Cu^{2+}:peptide molar ratio controls the final aggregation state of Aβ, with amyloid material predominating at sub-equimolar ratios and Cu^{2+} induced aggregate predominating at supra-equimolar ratios. The switch between the two aggregate forms is centered at an equimolar ratio where both forms of the peptide can be seen to coexist. We have demonstrated that Cu^{2+} induced aggregation results in the formation of both small spherical and large amorphous aggregates. Once formed, the Cu^{2+} induced aggregates are unable to influence the rate of amyloid formation and do not convert into amyloid material over the course of several weeks. Aged Cu^{2+} bound forms of Aβ are shown to be highly toxic to neuronal cells. In addition, only the Cu^{2+} induced aggregates produce large amounts of the oxidative stress marker dityrosine, and this marker is only observed post aggregate formation. These Cu^{2+} induced aggregates characterized here may well represent the metal mediated toxic species of Aβ (*8*, *48*, *49*). The clinical importance of our current studies is that the definition of the Aβ:Cu^{2+} species can significantly advance the development of metal protein attenuating compounds, which target the Aβ:Cu^{2+} complex, as effective AD therapeutics (*9*, *14*).

SUPPORTING INFORMATION AVAILABLE

Supplementary Figure 1; showing the dissociation of the large amyloid-like aggregates prepared in the absence of Cu^{2+} by Gdn.SCN. Supplementary Figure 2; Long-term growth of Aβ1−42 at 10 μM a Cu^{2+}:peptide molar ratio of 2.5:1 monitored by ThT fluorescence and EM. This material is available free of charge via the Internet at http://pubs.acs.org.

REFERENCES

1. Masters, C. L., Cappai, R., Barnham, K. J., and Villemagne, V. L. (2006) Molecular mechanisms for Alzheimer's disease: Implications for neuroimaging and therapeutics, *J. Neurochem. 97*, 1700−1725.
2. Bush, A. I. (2003) The metallobiology of Alzheimer's disease, *Trends Neurosci. 26*, 207−214.
3. Lovell, M. A., Robertson, J. D., Teesdale, W. J., Campbell, J. L., and Markesbery, W. R. (1998) Copper, iron and zinc in Alzheimer's disease senile plaques, *J. Neurol. Sci. 158*, 47−52.
4. Lee, J. Y., Mook-Jung, I., and Koh, J. Y. (1999) Histochemically reactive zinc in plaques of the Swedish mutant beta-amyloid precursor protein transgenic mice, *J. Neurosci. 19*, 1−5.
5. Suh, S. W., Jensen, K. B., Jensen, M. S., Silva, D. S., Kesslak, P. J., Danscher, G., and Frederickson, C. J. (2000) Histochemically-reactive zinc in amyloid plaques, angiopathy, and degenerating neurons of Alzheimer's diseased brains, *Brain Res. 852*, 274−278.
6. Kardos, J., Kovacs, I., Hajos, F., Kalman, M., and Simonyi, M. (1989) Nerve endings from rat brain tissue release copper upon depolarization. *A* possible role in regulating neuronal excitability, *Neurosci. Lett. 103*, 139−144.
7. Butterfield, D. A., and Boyd-Kimball, D. (2004) Amyloid β-peptide(1−42.) contributes to the oxidative stress and neurodegeneration found in Alzheimer disease brain, *Brain Pathol. 14*, 426−432.
8. Huang, X., Atwood, C. S., Hartshorn, M. A., Multhaup, G., Goldstein, L. E., Scarpa, R. C., Cuajungco, M. P., Gray, D. N., Lim, J., Moir, R. D., Tanzi, R. E., and Bush, A. I. (1999) The A beta peptide of Alzheimer's disease directly produces hydrogen peroxide through metal ion reduction, *Biochemistry 38*, 7609−7616.
9. Barnham, K. J., Masters, C. L., and Bush, A. I. (2004) Neurodegenerative diseases and oxidative stress, *Nat. Rev. Drug Discov. 3*, 205−214.
10. Dai, X. L., Sun, Y. X., and Jiang, Z. F. (2006) Cu(II) potentiation of Alzheimer Abeta1−40. cytotoxicity and transition on its secondary structure, *Acta Biochim. Biophys. Sin. (Shanghai) 38*, 765−772.
11. Sayre, L. M., Perry, G., Harris, P. L., Liu, Y., Schubert, K. A., and Smith, M. A. (2000) *In situ* oxidative catalysis by neurofibrillary tangles and senile plaques in Alzheimer's disease: a central role for bound transition metals, *J. Neurochem. 74*, 270−279.
12. Cherny, R. A., Legg, J. T., McLean, C. A., Fairlie, D. P., Huang, X., Atwood, C. S., Beyreuther, K., Tanzi, R. E., Masters, C. L., and Bush, A. I. (1999) Aqueous dissolution of Alzheimer's disease Abeta amyloid deposits by biometal depletion, *J. Biol. Chem. 274*, 23223−23228.
13. Cherny, R. A., Atwood, C. S., Xilinas, M. E., Gray, D. N., Jones, W. D., McLean, C. A., Barnham, K. J., Volitakis, I., Fraser, F. W., Kim, Y., Huang, X., Goldstein, L. E., Moir, R. D., Lim, J. T., Beyreuther, K., Zheng, H., Tanzi, R. E., Masters, C. L., and Bush, A. I. (2001) Treatment with a copper-zinc chelator markedly and rapidly inhibits beta-amyloid accumulation in Alzheimer's disease transgenic mice, *Neuron 30*, 665−676.
14. Ritchie, C. W., Bush, A. I., Mackinnon, A., Macfarlane, S., Mastwyk, M., MacGregor, L., Kiers, L., Cherny, R., Li, Q. X., Tammer, A., Carrington, D., Mavros, C., Volitakis, I., Xilinas, M., Ames, D., Davis, S., Beyreuther, K., Tanzi, R. E., and Masters, C. L. (2003) Metal-protein attenuation with iodochlorhydroxyquin (clioquinol) targeting Abeta amyloid deposition and toxicity in Alzheimer disease: a pilot phase 2 clinical trial, *Arch. Neurol. 60*, 1685−1691.
15. Cuajungco, M. P., Goldstein, L. E., Nunomura, A., Smith, M. A., Lim, J. T., Atwood, C. S., Huang, X., Farrag, Y. W., Perry, G., and Bush, A. I. (2000) Evidence that the beta-amyloid plaques of Alzheimer's disease represent the redox-silencing and entombment of abeta by zinc, *J. Biol. Chem. 275*, 19439−19442.
16. Huang, X., Cuajungco, M. P., Atwood, C. S., Hartshorn, M. A., Tyndall, J. D., Hanson, G. R., Stokes, K. C., Leopold, M.,

Multhaup, G., Goldstein, L. E., Scarpa, R. C., Saunders, A. J., Lim, J., Moir, R. D., Glabe, C., Bowden, E. F., Masters, C. L., Fairlie, D. P., Tanzi, R. E., and Bush, A. I. (1999) Cu(II) potentiation of Alzheimer Aβ neurotoxicity: correlation with cell-free hydrogen peroxide production and metal reduction, *J. Biol. Chem. 274*, 37111−37116.

17. Smith, D. P., Smith, D. G., Curtain, C. C., Boas, J. F., Pilbrow, J. R., Ciccotosto, G. D., Lau, T. L., Tew, D. J., Perez, K., Wade, J. D., Bush, A. I., Drew, S. C., Separovic, F., Masters, C. L., Cappai, R., and Barnham, K. J. (2006) Copper-mediated amyloid-beta toxicity is associated with an intermolecular histidine bridge, *J. Biol. Chem. 281*, 15145−14154.
18. Crouch, P. J., Blake, R., Duce, J. A., Ciccotosto, G. D., Li, Q. X., Barnham, K. J., Curtain, C. C., Cherny, R. A., Cappai, R., Dyrks, T., Masters, C. L., and Trounce, I. A. (2005) Copper-dependent inhibition of human cytochrome c oxidase by a dimeric conformer of amyloid-beta1−42, *J. Neurosci. 25*, 672−679.
19. Curtain, C. C., Ali, F., Volitakis, I., Cherny, R. A., Norton, R. S., Beyreuther, K., Barrow, C. J., Masters, C. L., Bush, A. I., and Barnham, K. J. (2001) Alzheimer's disease amyloid-beta binds copper and zinc to generate an allosterically ordered membrane-penetrating structure containing superoxide dismutase-like subunits, *J. Biol. Chem. 276*, 20466−20473.
20. Karr, J. W., Kaupp, L. J., and Szalai, V. A. (2004) Amyloid-beta binds Cu^{2+} in a mononuclear metal ion binding site, *J. Am. Chem. Soc. 126*, 13534−13538.
21. Antzutkin, O. N. (2004) Amyloidosis of Alzheimer's Abeta peptides: solid-state nuclear magnetic resonance, electron para-magnetic resonance, transmission electron microscopy, scanning transmission electron microscopy and atomic force microscopy studies, *Magn. Reson. Chem. 42*, 231−246.
22. Syme, C. D., Nadal, R. C., Rigby, S. E., and Viles, J. H. (2004) Copper binding to the amyloid-beta (Abeta) peptide associated with Alzheimer's disease, *J. Biol. Chem. 279*, 18169−18177.
23. Karr, J. W., Akintoye, H., Kaupp, L. J., and Szalai, V. A. (2005) N-Terminal deletions modify the Cu2+ binding site in amyloid-beta, *Biochemistry 44*, 5478−5487.
24. Atwood, C. S., Moir, R. D., Huang, X. D., Scarpa, R. C., Bacarra, N. M. E., Romano, D. M., Hartshorn, M. K., Tanzi, R. E., and Bush, A. I. (1998) Dramatic aggregation of Alzheimer abeta by Cu(II) is induced by conditions representing physiological acidosis, *J. Biol. Chem. 273*, 12817−12826.
25. Klug, G. M., Losic, D., Subasinghe, S. S., Aguilar, M. I., Martin, L. L., and Small, D. H. (2003) Beta-amyloid protein oligomers induced by metal ions and acid pH are distinct from those generated by slow spontaneous ageing at neutral pH, *Eur. J. Biochem. 270*, 4282−4293.
26. Raman, B., Ban, T., Yamaguchi, K. I., Sakai, M., Kawai, T., Naiki, H., and Goto, Y. (2005) Metal ion-dependent effects of clioquinol on the fibril growth of an amyloid {beta} peptide, *J. Biol. Chem. 280*, 16157−16162.
27. Atwood, C. S., Scarpa, R. C., Huang, X., Moir, R. D., Jones, W. D., Fairlie, D. P., Tanzi, R. E., and Bush, A. I. (2000) Characterization of copper interactions with Alzheimer amyloid beta peptides: identification of an attomolar-affinity copper binding site on amyloid β1−42, *J. Neurochem. 75*, 1219−1233.
28. Pajonk, F. G., Kessler, H., Supprian, T., Hamzei, P., Bach, D., Schweickhardt, J., Herrmann, W., Obeid, R., Simons, A., Falkai, P., Multhaup, G., and Bayer, T. A. (2005) Cognitive decline correlates with low plasma concentrations of copper in patients with mild to moderate Alzheimer's disease, *J. Alzheimers Dis. 8*, 23−27.
29. Squitti, R., Pasqualetti, P., Dal Forno, G., Moffa, F., Cassetta, E., Lupoi, D., Vernieri, F., Rossi, L., Baldassini, M., and Rossini, P. M. (2005) *E*xcess of serum copper not related to ceruloplasmin in Alzheimer disease, *Neurology 64*, 1040−1046.
30. Ciccotosto, G. D., Tew, D., Curtain, C. C., Smith, D., Carrington, D., Masters, C. L., Bush, A. I., Cherny, R. A., Cappai, R., and Barnham, K. J. (2004) Enhanced toxicity and cellular binding of a modified amyloid beta peptide with a methionine to valine substitution, *J. Biol. Chem. 279*, 42528−42534.
31. Ida, N., Hartmann, T., Pantel, J., Schroder, J., Zerfass, R., Forstl, H., Sandbrink, R., Masters, C. L., and Beyreuther, K. (1996) Analysis of heterogeneous A4 peptides in human cerebrospinal fluid and blood by a newly developed sensitive Western blot assay, *J. Biol. Chem. 271*, 22908−22914.
32. Bitan, G., Kirkitadze, M. D., Lomakin, A., Vollers, S. S., Benedek, G. B., and Teplow, D. B. (2003) *A*myloid beta -protein (Abeta) assembly: A beta 40 and A beta 42 oligomerize through distinct pathways, *Proc. Natl. Acad. Sci. U.S.A. 100*, 330−335.
33. Chromy, B. A., Nowak, R. J., Lambert, M. P., Viola, K. L., Chang, L., Velasco, P. T., Jones, B. W., Fernandez, S. J., Lacor, P. N., Horowitz, P., Finch, C. E., Krafft, G. A., and Klein, W. L. (2003) Self-assembly of Abeta1−42. into globular neurotoxins, *Biochemistry 42*, 12749−12760.
34. Walsh, D. M., Lomakin, A., Benedek, G. B., Condron, M. M., and Teplow, D. B. (1997) Amyloid beta-protein fibrillogenesis. Detection of a protofibrillar intermediate, *J. Biol. Chem. 272*, 22364−22372.
35. LeVine, H., 3rd. (2004) Alzheimer's beta-peptide oligomer formation at physiologic concentrations, *Anal. Biochem. 335*, 81−90.
36. Bush, A. I., Pettingell, W. H., Jr., Paradis, M. D., and Tanzi, R. E. (1994) Modulation of A beta adhesiveness and secretase site cleavage by zinc, *J. Biol. Chem. 269*, 12152−12158.
37. Harper, J. D., and Lansbury, P. T. (1997) *M*odels of amyloid seeding in Alzheimier's disease and scrapie: mechanistic truths and physiological consequences of the time-dependent solubility of amyloid proteins, *Annu. Rev. Biochem. 66*, 385−407.
38. Atwood, C. S., Perry, G., Zeng, H., Kato, Y., Jones, W. D., Ling, K. Q., Huang, X., Moir, R. D., Wang, D., Sayre, L. M., Smith, M. A., Chen, S. G., and Bush, A. I. (2004) Copper mediates dityrosine cross-linking of Alzheimer's amyloid-beta, *Biochemistry 43*, 560−568.
39. Barnham, K. J., Haeffner, F., Ciccotosto, G. D., Curtain, C. C., Tew, D., Mavros, C., Beyreuther, K., Carrington, D., Masters, C. L., Cherny, R. A., Cappai, R., and Bush, A. I. (2004) Tyrosine gated electron transfer is key to the toxic mechanism of Alzheimer's disease beta-amyloid, *Faseb J. 18*, 1427−1429.
40. Bitan, G., Tarus, B., Vollers, S. S., Lashuel, H. A., Condron, M. M., Straub, J. E., and Teplow, D. B. (2003) A molecular switch in amyloid assembly: Met35 and amyloid beta-protein oligomerization, *J. Am. Chem. Soc. 125*, 15359−15365.
41. Barnham, K. J., Ciccotosto, G. D., Tickler, A. K., Ali, F. E., Smith, D. G., Williamson, N. A., Lam, Y. H., Carrington, D., Tew, D., Kocak, G., Volitakis, I., Separovic, F., Barrow, C. J., Wade, J. D., Masters, C. L., Cherny, R. A., Curtain, C. C., Bush, A. I., and Cappai, R. (2003) Neurotoxic, redox-competent Alzheimer's beta-amyloid is released from lipid membrane by methionine oxidation, *J. Biol. Chem. 278*, 42959−42965.
42. Yoburn, J. C., Tian, W., Brower, J. O., Nowick, J. S., Glabe, C. G., and Van Vranken, D. L. (2003) Dityrosine cross-linked Abeta peptides: fibrillar beta-structure in Abeta(1−40.) is conducive to formation of dityrosine cross-links but a dityrosine cross-link in Abeta(8−14.) does not induce beta-structure, *Chem. Res. Toxicol. 16*, 531−535.
43. Galeazzi, L., Ronchi, P., Franceschi, C., and Giunta, S. (1999) In vitro peroxidase oxidation induces stable dimers of beta-amyloid (1−42) through dityrosine bridge formation, *Amyloid 6*, 7−13.
44. Curtain, C. C., Barnham, K. J., and Bush, A. I. (2003) Abeta metallobiology and the development of novel metal-protein attenuating compounds (MPACs) for Alzheimer's disease, *Curr. Med. Chem.: Immunol., Endocr. Metab. Agents 3*, 309−315.
45. Huang, X., Atwood, C. S., Moir, R. D., Hartshorn, M. A., Tanzi, R. E., and Bush, A. I. (2004) Trace metal contamination initiates the apparent auto-aggregation, amyloidosis, and oligomerization of Alzheimer's Abeta peptides, *J. Biol. Inorg. Chem. 9*, 954−960.
46. Roher, A. E., Chaney, M. O., Kuo, Y. M., Webster, S. D., Stine, W. B., Haverkamp, L. J., Woods, A. S., Cotter, R. J., Tuohy, J. M., Krafft, G. A., Bonnell, B. S., and Emmerling, M. R. (1996) Morphology and toxicity of Abeta-(1−42.) dimer derived from neuritic and vascular amyloid deposits of Alzheimer's disease, *J. Biol. Chem. 271*, 20631−20635.
47. Maynard, C. J., Bush, A. I., Masters, C. L., Cappai, R., and Li, Q. X. (2005) Metals and amyloid-beta in Alzheimer's disease, *Int. J. Exp. Pathol. 86*, 147−159.
48. Opazo, C., Huang, X., Cherny, R. A., Moir, R. D., Roher, A. E., White, A. R., Cappai, R., Masters, C. L., Tanzi, R. E., Inestrosa, N. C., and Bush, A. I. (2002) Metalloenzyme-like activity of Alzheimer's disease beta-amyloid. Cu-dependent catalytic conversion of dopamine, cholesterol, and biological reducing agents to neurotoxic H(2)O(2), *J. Biol. Chem. 277*, 40302−40308.
49. Behl, C., Davis, J. B., Lesley, R., and Schubert, D. (1994) Hydrogen peroxide mediates amyloid beta protein toxicity, *Cell 77*, 817−827.

50. Bocharova, O. V., Breydo, L., Salnikov, V. V., and Baskakov, I. V. (2005) Copper(II) inhibits in vitro conversion of prion protein into amyloid fibrils, *Biochemistry 44*, 6776−6787.
51. Rasia, R. M., Bertoncini, C. W., Marsh, D., Hoyer, W., Cherny, D., Zweckstetter, M., Griesinger, C., Jovin, T. M., and Fernandez, C. O. (2005) Structural characterization of copper(II) binding to alpha-synuclein: Insights into the bioinorganic chemistry of Parkinson's disease, *Proc. Natl. Acad. Sci. U.S.A. 102*, 4294−4299.

BI0620961